Observation of two species of vortices in the anisotropic spin-triplet superconductor Sr_2RuO_4

V. O. Dolocan,[1,*] P. Lejay,[1] D. Mailly,[2] and K. Hasselbach[1]
[1]*CRTBT-CNRS, 25 Avenue des Martyrs, 38042 Grenoble, France*
[2]*LPN-CNRS, Route de Nozay, 91460 Marcoussis, France*
(Received 30 June 2006; published 6 October 2006)

Magnetic-flux structures in single crystals of the layered spin-triplet superconductor Sr_2RuO_4 are studied by scanning μSQUID force microscopy. Vortex chains appear as the applied field is tilted along the in-plane direction of the superconductor. The vortex chains align along the direction of the in-plane component of the applied magnetic field. The decoration of in-plane vortices by crossing Abrikosov vortices is observed: two vortex orientations are apparent simultaneously, one along the layers and the other perpendicular to the layers. The crossing vortices appear preferentially on the in-plane vortices.

DOI: 10.1103/PhysRevB.74.144505 PACS number(s): 74.20.Rp, 74.25.Qt, 74.70.Pq, 85.25.Dq

I. INTRODUCTION

The magnetic properties of superconductors depend strongly on their crystalline and electronic anisotropy. Prominent examples are the high-temperature superconductors. Intense research efforts have revealed a variety of vortex phenomena in these compounds (vortex glass, vortex meltin crossing of Josephson vortices by pancake vortices). The general theoretical approach on vortex matter is based on the anisotropic Ginzburg-Landau (GL) theory. There the anisotropy is expressed in terms of the effective mass of the electron. For layered anisotropic superconductors, the out-of-plane effective mass m_c is much larger than the in-plane effective masses ($m_c \gg m_{ab}$). To describe this anisotropy the parameter $\gamma=(m_c/m_{ab})^{1/2}=\lambda_c/\lambda_{ab}$ (Ref. 1) is used. For example, $NbSe_2$, $\gamma=3.3$; YBCO, $\gamma=5-8$; and BSCCO, γ is higher than 150—γ being dependent on the oxygen doping of the high-T_c superconductors.

In moderately anisotropic superconductors, when the magnetic field is tilted away from the anisotropy axis, calculations based on GL theory show that the screening currents tend to flow in approximately elliptical paths around the vortex cores and parallel to the layers.[2,3] This current flow creates a net transverse magnetization and attraction appears between the tilted vortices, leading finally to the development of vortex chains formed by inclined vortices. These vortex chains have been observed in YBCO.[4]

In highly anisotropic superconductors, Josephson vortices appear if the distance between the layers is larger than ξ_c. The Josephson vortices are confined in the space between the layers. The Lawrence-Doniach (LD) model is used as the continuous GL theory cannot be applied anymore. In the LD model the tilted vortex is described as a tilted stack of two-dimensional (2D) pancake vortices connected by Josephson strings. Pancake vortices are characterized by a circular supercurrent pattern flowing in the layers and Josephson strings being short segments of Josephson vortices confined to the insulating region between the superconducting layers. High-T_c superconductors with a weak interlayer coupling such as BSCCO, are treated as 2D superconductors according to the Lawrence-Doniach model. Magnetic imaging of vortices was quintessential for the experimental exploration of vortex structures in BSCCO: Bitter decoration experiments revealed vortex chains separated by a vortex lattice;[5] scanning Hall probe microscopy showed Josephson vortices decorated by pancake vortices.[6,7]

In the present study vortex matter is investigated in the anisotropic layered superconductor Sr_2RuO_4. The superconducting transition temperature of Sr_2RuO_4 is of the order of 1.45 K.[8] Like high-T_c cuprates, the tetragonal Sr_2RuO_4 has a layered structure and the RuO_2 planes are separated by 12.74 Å and have highly anisotropic properties.[9] Sr_2RuO_4 has a γ value of 20 situating it between YBCO and BSCCO on the anisotropy scale. We expect Sr_2RuO_4 to act more like a three-dimensional (3D) superconductor as the c-axis parameter is 3 times smaller than the coherence length ξ_c. The Ginzburg-Landau parameter $\kappa=\lambda/\xi$ is around 2.3 when the magnetic field is applied along the c-axis direction and 46 for the in-plane direction. The physical properties of Sr_2RuO_4 are very rich and indications accumulated showing that it might exhibit unconventional superconductivity.[10–12] A coherent picture can be obtained in terms of a superconducting state characterized by the breaking of the time-reversal symmetry and requiring a multicomponent order parameter of p-wave symmetry with a gap function $d=\hat{z}(k_x \pm ik_y)$. The symmetry of the order parameter should give rise to domains of opposite chirality, $\hat{z}(k_x+ik_y)$ and $\hat{z}(k_x-ik_y)$ separated by domain walls, the formation of fractional vortices on the domain walls, and should generate spontaneous currents at the edges of the crystal. It was conjectured that domain walls might be preferential pinning sites for vortices.[13] Magnetic microscopy is a means of choice to study the relevance of these predictions. Vortices along with vortex coalescence were observed in Sr_2RuO_4 by μSQUID magnetic microscopy.[14] Here we focus on vortex matter in Sr_2RuO_4, demonstrating the presence of tilted vortex chains in, and evidencing pinning of perpendicular vortices on in-plane vortex chains in Sr_2RuO_4, making Sr_2RuO_4 the first anisotropic 3D superconductor presenting crossing vortices.

We use for magnetic imaging a high-resolution scanning μSQUID microscope[15] (SμSM) working in a dilution refrigerator. The SμSM has an aluminum μSQUID as a pickup loop of 1.2 μm diameter. The critical current of the μSQUID is a periodic function of the magnetic flux emerging perpendicularly from the sample surface. The images shown are maps of the critical-current value of the μSQUID scanning

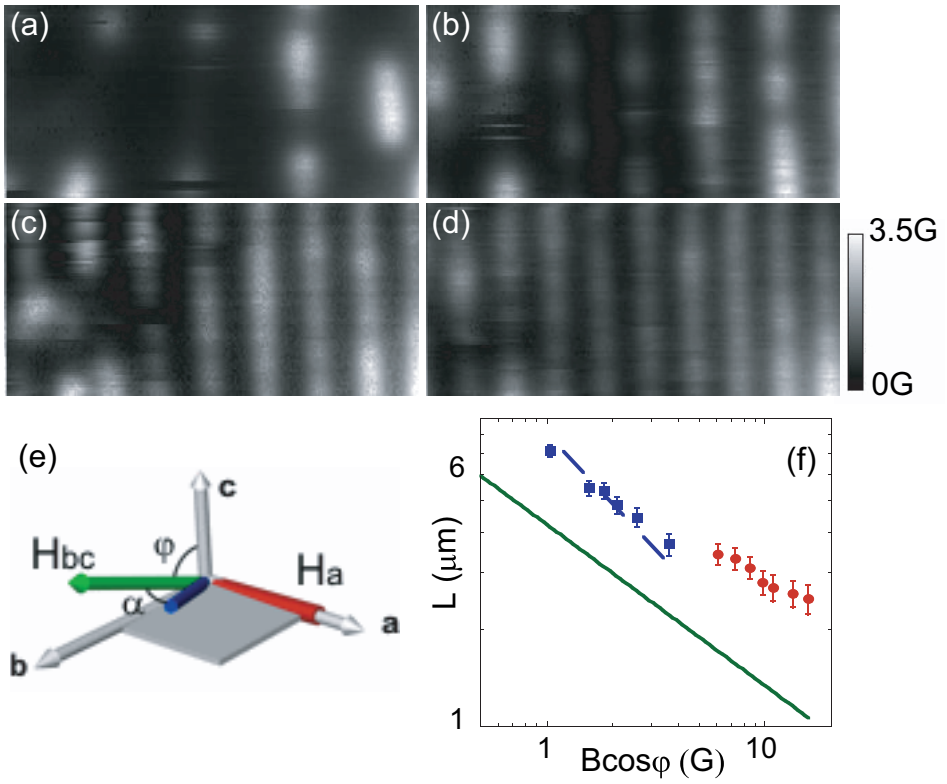

FIG. 1. (Color online) Scanning μSQUID microscope images of the magnetic flux above the *ab* face of Sr_2RuO_4 at $T=0.35$ K. During field cooling the magnetic field is applied at a fixed angle $\varphi=87°$ from the *c* axis varying for each panel as (a) 20 G, (b) 35 G, (c) 60 G, and (d) 70 G. The image area is 31 μm$\times$15 μm. The magnetic scale is shown on the right. (e) Scheme of the two applied magnetic fields. The magnetic field H_{bc} can be rotated with an angle φ from the *c* axis (in the *bc* plane). A second fixed magnetic field H_a can be applied in plane. The resultant field is also shown schematically. (f) Interchain distance as a function of the normal field. The points are fitted with a B^{-1} law. The line represents the isotropic limit $B^{-1/2}$.

the surface. We used two different high-quality crystals coming from the same rod showing volume superconductivity below a temperature of 1.31 K. The two samples are large plates with a thickness of 0.5 and 0.6 mm. The surface is cleaved and atomic force microscopy (AFM) images show flatness down to the order of 6 Å. The magnetic fields are applied by a solenoid and a rotatable Helmholtz coil; the coils are at room temperature. The solenoid axis is parallel to the *ab* face of the sample [H_a in Fig. 1(e)] and the Helmholtz coil generates a field H_{bc} perpendicular to the solenoid axis. Adjusting the relative angle and the magnitude of the two fields allows us to point the resultant field along any direction.

II. VORTEX CHAINS IN Sr_2RuO_4

Vortex chains form in Sr_2RuO_4 (Ref. 16) at low fields and tilt angles higher than 70° from the *c* axis. In Fig. 1 only a field H_{bc} was applied at an angle φ of 87° from the *c* axis and the magnetic flux was increased from 0 to 70 G. Each measurement was acquired after a field-cooling procedure. The vortex chains start to appear in our images for fields higher than 20 G, $2H_{c1}$ for the in-plane direction of our sample. As the field is increased the chain density increases also. When the number of vortices reaches an equilibrium value in each chain the formation of a new chain becomes energetically favorable.

Calculations in the GL theory in the London limit[17] show that the intrachain distance between vortices remains constant with an increasing field while the interchain distance decreases like B^{-1}. This distance can be calculated in the single-chain limit and, using the parameters of Sr_2RuO_4, the vortex-vortex intrachain distance yields $2\lambda_{ab}\sim 0.3$ μm, lower than our SQUID resolution. On the other hand, we can measure the interchain distance between the chains and compare it with the GL theory. In our experiment on Sr_2RuO_4, at low perpendicular fields the distance between the chains follows the B^{-1} dependence as in the GL theory [Fig. 1(f), fitted points], though the value of the observed spacing is larger than predicted. As the field increases, the distance between the chains should tend monotonously to the isotropic limit (the line, $B^{-1/2}$ dependence). A regular square lattice is observed by small angle neutron scattering (SANS) for fields higher than 50 G applied along the *c* axis. With an increasing perpendicular field, we observe that the interchain distance deviates from the B^{-1} dependence characteristic of vortex chains [Fig. 1(f), points not fitted]. The chains seem to accommodate a higher density of vortices than predicted by the London theory, retarding the formation of the vortex lattice. This finding is consistent with vortex coalescence[14] in Sr_2RuO_4 at intermediate magnetic fields applied parallel to the *c* axis.

Ginzburg-Landau theory predicts that the vortex chains are aligned in the plane spanned by the crystal's anisotropy axis and the applied field. When the applied field is rotated in the *ab* plane, the vortex chains should follow. We undertook these measurements on the second crystal in turning the in-plane component of the field vector by an angle α relative to the *bc* plane. The field was applied in superposing two fields: H_a oriented along the *a* axis, and the field in the *bc* plane H_{bc} tilted from the *c* axis by the angle φ. Each measurement was done after field cooling (Fig. 2). We varied the direction α of the in-plane component from 0° to 90°. The linear-vortex chains align with the in-plane direction of the applied field as expected. The features in the magnetic images that are fixed

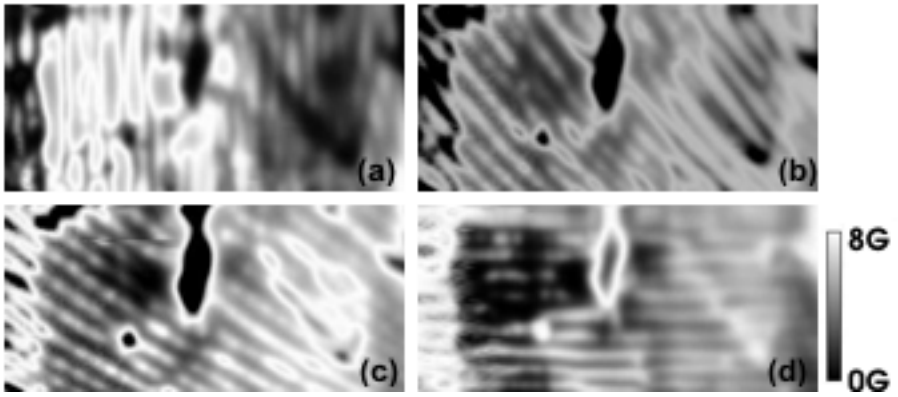

FIG. 2. Rotation of the vortex chains in Sr_2RuO_4. When the amplitudes of the two different magnetic fields are varied the angle α of the resultant field is changed: (a) H_{bc}=54 G, φ=80°, α=0°; (b) H_{bc}=54 G, H_a=54 G, φ=85°, α=45°; (c) H_{bc}=39.3 G, H_a=68 G, φ=85°, α=60°; (d) H_{bc}=−6 G, H_a=90 G, φ=0°, α=90°. All images are taken after field cooling at a temperature of 0.6 K. The dimensions of each image are 62 μm×30 μm.

are due to flux pinning at surface asperities. In panel (a) the broadened flux lines are attributed to the simultaneous presence of vortex chains and vortex coalescence, fostered by a perpendicular field of 9 G. For some values of the perpendicular field the vortices in chains are well separated like in image (c) when the perpendicular field is of the order of 3.5 G. These single vortices seem to be pinned on the vortex chains, reminiscent of the decoration of Josephson vortices by pancake vortices observed in the 2D superconductor BSCCO. Exploring the history dependence of the magnetic-field penetration in the crystal allows us to examine this state in the anisotropic 3D superconductor in more detail.

III. CROSSING VORTICES IN Sr_2RuO_4

In order to explore the vortex pinning and the vortex-chain mechanism in Sr_2RuO_4 we undertook measurements changing the applied magnetic field while the sample is in the superconducting state. The magnetic field component parallel to the plane is higher than the first critical field H_{c1} in the in-plane direction (H_{c1}^{ab}=10 G), while the perpendicular component is lower than H_{c1} (H_{c1}^{c}=50 G). In a first approximation a formation of tilted vortex chains might be expected as shown in the field-cooled case (see Fig. 1). With magnetic fields close to the *ab* plane for different field preparations we observe vortices decorating flux channels. We observe also a tendency for a long-range anticorrelation between decorating vortices in adjacent chains, reminding us of a distorted hexagonal lattice. This anticorrelation may be a sign that the vortex pinning on the chains is weak. Zero-field cooling (ZFC) [Figs. 3(a)–3(c)] and field cooling (FC) [Fig. 1(c)] sample preparation results in different vortex configurations: we observe the decoration of flux channels mostly in the ZFC experiments. Due to the lower first-critical field the magnetic flux penetrates preferentially along the planes, forming the flux channels, and the perpendicular vortices are pinned on the flux channels. In the FC experiments for a wide range of angles the flux expulsion happens in such a way that only tilted vortices appear in the sample. In Fig. 2(c) aligned vortices can be seen. The distinction of chains of tilted vortices and flux channels along the planes is made considering the amplitude of the signal. As shown by the magnetic scales on the right of each image in Fig. 3, in the images (a)–(c) the vortices have a similar magnetic amplitude as the vortices present when the field is applied along the *c* axis.[14] A normal component of the field of the order of 0.4 G creates these vortices. In the FC case [Fig. 1(c)] the magnetic flux coming out of the sample has a much larger amplitude as if the vortices would be closer together. We should have around 70 vortices in the image for the FC case, but the vortices appear as tilted vortices forming a vortex chain. All the images in Fig. 1 and Figs. 3(a)–3(c) are taken at the same place in the sample. We observe also that the decorating vortices have an oval shape [Fig. 3(d)], similar to

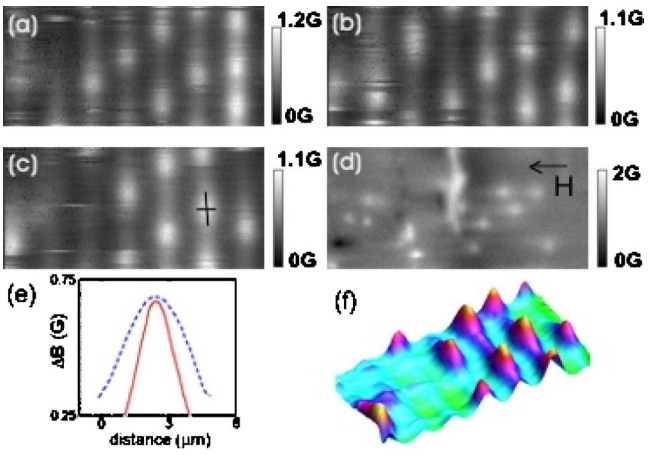

FIG. 3. (Color online) Crossing vortices in Sr_2RuO_4. The (a)–(c) images are taken after different field preparations: (a) 50 G ZFC; (b) 5 G FC and increased to 50 G at low temperature; (c) 10 G FC and increased to 50 G at low *T*. The magnetic scale for each image is shown on the right. The dimensions are 31 μm×15 μm and the imaging temperature is 0.35 K. The tilting angle is 87°. (d) 68 G FC with the field applied only in plane (indicated by an arrow). A "halo" around each perpendicular vortex is visible. The dimensions of the image are 62 μm×30 μm. (e) Two perpendicular line scans at one of the decorating vortices [indicated by a cross in panel (c)]. The image (f) is the 3D representation of the image (c).

the pancake vortices decorating Josephson vortices.[18] In the case of BSCCO the deformation is explained by a displacement of the pancake vortices due to circulating currents of the Josephson vortices.[19] In a similar manner the interaction between in-plane flux channels and the crossing vortices may result in the elongated shape of the decorating vortices detected by the SQUID. The perpendicular vortices appear due to a small residual field estimated to be 0.15 G. The deformation of the vortex shape is a sign for the strong interaction between the two species of vortices and confirms the finding that the crossing vortices are pinned on the flux channels running along the layers.

IV. DISCUSSION

In isotropic superconductors at low tilted fields the flux lines penetrate parallel to each other and with the average field in the sample and arrange themselves in a pattern that minimizes the interaction energy. If the superconductor is strongly anisotropic the free energy of the vortex state has two local minima and consequently a flux line can penetrate in two distinct directions in the material. For high anisotropy only flux lines that are nearly parallel or perpendicular to the layers are stable.[20,21] In the LD model this corresponds to the separation in pancake vortices and Josephson vortices. The distance between the Josephson vortices is given by[19]

$$L = \sqrt{\sqrt{3}\gamma\phi_0/(2B_{ab})}, \tag{1}$$

where B_{ab} is the in-plane field (parallel field) and ϕ_0 is the quantum of flux. In Sr_2RuO_4 this distance should correspond to the interchain distance supposing the LD model applies. In Fig 4(c) the interchain distance is shown as a function of $B_{ab}^{-1/2}$. The dashed line passing through the measured points represents the theoretical values calculated with the formula (1) for an anisotropy parameter $\gamma=28$. The line represents the theoretical calculation for $\gamma=20$, which corresponds to the values found in the literature.[9] The anisotropy parameter γ is determined from the ratio of the critical fields or penetration depths. Values of 15–20 were found also by μSQUID microscopy, imaging the *ac* face of the crystal and determining the deformation of the vortex (images not shown). As the superconductivity is thought to be orbital dependent,[22] the anisotropy parameter could vary (giving rise to two different penetration depths) and an anisotropy parameter value of 28 might be plausible. The structures observed would then correspond to pancake vortices pinned on Josephson vortices [Fig. 4(b)]. However, Sr_2RuO_4 should act more like a 3D superconductor as the coherence length is three times longer than the interlayer spacing. This makes the observed decoration of in-plane flux channels by crossing vortices unique.

The presence of Josephson vortices is not a necessary prerequisite for the presence of crossing vortices: in the classical London theory two parallel vortices repel each other. This repulsion is maintained if one tilts one of the vortices from the common direction. The interaction energy is given by $E_{int}=\frac{\phi_0^2}{2\mu_0\lambda_{ab}}\cot(\alpha)\exp\left(-\frac{d}{\lambda_{ab}}\right)$, where d is the smallest distance between vortices and α is the angle between them.[23]

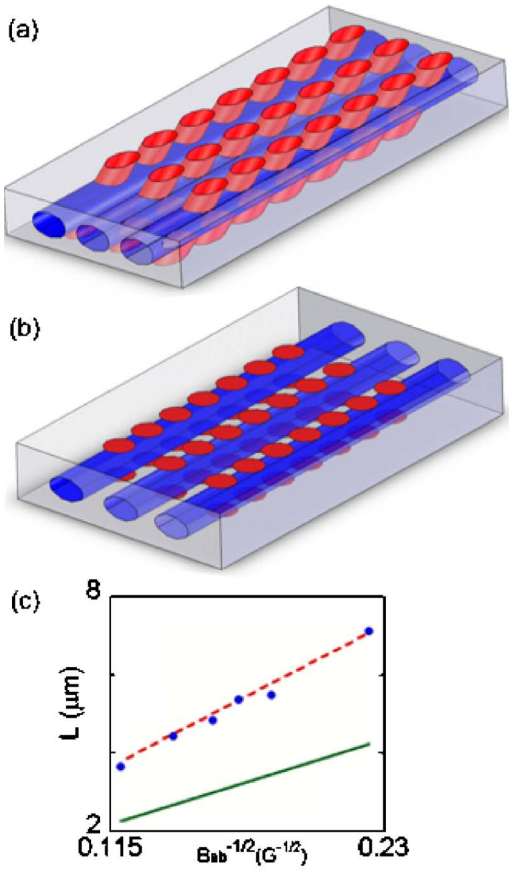

FIG. 4. (Color online) Scheme of interpenetrating vortices: (a) tilted vortices and (b) pancake vortices crossing Josephson vortices. (c) The interchain distance as a function of the in-plane component of the field $B_{ab}^{-1/2}$, supposing the applicability of the Lawrence-Doniach model. The dashed line represents the theoretical values of the interchain distance calculated from Eq. (1) with $\gamma=28$. The line represents the values calculated with $\gamma=20$.

When the angle between vortices becomes 90° the flux lines do not interact. If the angle increases more the flux lines start to attract each other and the highest attraction energy is for the antiparallel direction. Daemen *et al.*[24] showed that the free energy of a mixed lattice formed by vortices parallel to the *c* axis and vortices inclined at some angle from the *c* axis is lower than the free energy of a deformed inclined lattice. This model predicted that two types of vortices may be observed in Sr_2RuO_4 formed by two interpenetrating lattices [Fig. 4(a)]; a lattice of vortices parallel to the layers and decorating vortices that are nearly parallel to the *c* axis.

V. CONCLUSION

We imaged two types of vortex configurations in the anisotropic spin-triplet superconductor Sr_2RuO_4. The first configuration consists of vortex chains formed by tilted vortices. The qualitative variation of the vortex-chain spacing is consistent with GL theory though the vortex spacing is closer than predicted. For higher perpendicular fields we see that the variation of the vortex-chain spacing is slower than predicted, resulting in a higher vortex density in the chain. This

accommodation of a higher vortex density may be related to the observed vortex coalescence in Sr_2RuO_4.

The second vortex configuration consists of in-plane flux channels crossed by perpendicular Abrikosov vortices. The observed deformation of the pinned Abrikosov vortices is a sign of the interaction between the Abrikosov vortices and the flux channels. The strong interlayer coupling of Sr_2RuO_4 excludes the existence of Josephson vortices in this compound, precluding the applicability of the Lawrence Doniach model of an interplay between Josephson vortices and pancake vortices, well established for crossing vortices observed in high-T_c superconductors. The possibility of crossing vortices is predicted in the case of sufficiently anisotropic 3D superconductors. We think that this is the case here. Our observations are qualitatively understood; for a more quantitative interpretation the theoretical models have yet to be developed taking into account the physical properties of Sr_2RuO_4, quite different from those of other anisotropic superconductors. We are shedding light on aspects of vortex physics in our exploration of vortex-chain formation and of flux channels decorated by vortices and, in particular, we show the richness of physical phenomena in Sr_2RuO_4. Sr_2RuO_4 is at the intersection of many different domains: unconventional superconductivity, anisotropy, and nonlocal electrodynamics of low-κ superconductors.

ACKNOWLEDGMENTS

We acknowledge the support of CNRS and fruitful discussions with Y. Liu, P. Rodière, and T. Prouvé.

*Present address: Max-Planck-Institute for Chemical Physics of Solids, 40 Nöthnitzer Str., 01187 Dresden, Germany.

[1] J. R. Clem, Supercond. Sci. Technol. **11**, 909 (1998).
[2] A. I. Buzdin and A. Yu. Simonov, Zh. Eksp. Teor. Fiz. **98**, 2074 (1990) [Sov. Phys. JETP **71**, 1165 (1990)].
[3] V. G. Kogan, Phys. Rev. B **24**, 1572 (1981).
[4] P. L. Gammel, D. J. Bishop, J. P. Rice, and D. M. Ginsberg, Phys. Rev. Lett. **68**, 3343 (1992).
[5] C. A. Bolle, P. L. Gammel, D. G. Grier, C. A. Murray, D. J. Bishop, D. B. Mitzi, and A. Kapitulnik, Phys. Rev. Lett. **66**, 112 (1991).
[6] A. Grigorenko, S. Bending, T. Tamegai, S. Ooi, and M. Henini, Nature (London) **414**, 728 (2001).
[7] S. J. Bending and M. J. W. Dodgson, J. Phys.: Condens. Matter **17**, R955 (2005).
[8] Y. Maeno, H. Hashimoto, K. Ioshida, S. Nishizaki, T. Fujita, J. Bednorz, and F. Lichtenberg, Nature (London) **372**, 532 (1994).
[9] A. P. Mackenzie and Y. Maeno, Rev. Mod. Phys. **75**, 657 (2003).
[10] K. Ishida, H. Mukuda, Y. Kitaoka, K. Asayama, Z. Q. Mao, Y. Mori, and Y. Maeno, Nature (London) **396**, 658 (1998).
[11] K. D. Nelson, Z. Q. Mao, Y. Maeno, and Y. Liu, Science **306**, 1151 (2004).
[12] G. M. Luke, Y. Fudamoto, K. M. Kojima, M. I. Larkin, J. Merrin, B. Nachumi, Y. J. Uemura, Y. Maeno, Z. Q. Mao, Y. Mori, H. Nakamura, and M. Sigrist, Nature (London) **394**, 558 (1998).
[13] M. Sigrist and D. F. Agterberg, Prog. Theor. Phys. **102**, 965 (1999).
[14] V. O. Dolocan, C. Veauvy, F. Servant, P. Lejay, K. Hasselbach, Y. Liu, and D. Mailly, Phys. Rev. Lett. **95**, 097004 (2005).
[15] C. Veauvy, D. Mailly, and K. Hasselbach, Rev. Sci. Instrum. **73**, 3825 (2002).
[16] V. O. Dolocan, C. Veauvy, Y. Liu, F. Servant, P. Lejay, K. Hasselbach, and D. Mailly, Physica C **404**, 140 (2004).
[17] L. L. Daemen, L. J. Campbell, and V. G. Kogan, Phys. Rev. B **46**, 3631 (1992).
[18] A. N. Grigorenko, S. J. Bending, I. V. Grigorieva, A. E. Koshelev, T. Tamegai, and S. Ooi, Phys. Rev. Lett. **94**, 067001 (2005).
[19] A. E. Koshelev, Phys. Rev. Lett. **83**, 187 (1999).
[20] D. A. Huse, Phys. Rev. B **46**, 8621 (1992).
[21] A. Sudbo, E. H. Brandt, and D. A. Huse, Phys. Rev. Lett. **71**, 1451 (1993).
[22] D. F. Agterberg, T. M. Rice, and M. Sigrist, Phys. Rev. Lett. **78**, 3374 (1997).
[23] A. Sudbo and E. H. Brandt, Phys. Rev. Lett. **67**, 3176 (1991).
[24] L. L. Daemen, L. J. Campbell, A. Yu. Simonov, and V. G. Kogan, Phys. Rev. Lett. **70**, 2948 (1993).